JOURNAL OF
EMERGING INVESTIGATORS

Article

Exploring the resonant vibration of a cello with the finite element method

Catherine Hung[1], Te-Cheng Su[2], Dino Ponnampalam[1]

[1] Kang Chiao International School - Taipei Campus, New Taipei City, Taiwan

[2] Department of Materials Science and Engineering, National Taiwan University, Taipei City, Taiwan

SUMMARY

Violins are precisely crafted to present their brilliant quality in sound that dates from 16th century Italy. The wood component's Young's modulus (*E*), the soundpost, and the bass bar play significant roles in the instrument's sound production. Yet, current acoustic research mostly focuses on violins. Therefore, this research aimed to investigate resonant vibration using a cello model. We hypothesized the structural changes in the soundpost and bass bar would lead to different eigenfrequencies, in which the original structure yields the highest value compared to the rest. To accurately reveal the secrets of cellos' acoustics, we conducted numerical and graphical simulations with the finite element method. We utilized the simulation tool to calculate the eigenfrequencies of altered structures with varying Young's modulus and positions of the soundpost, with or without the bass bar. We identified specific vibration mode shapes across all structures and found that Young's modulus had the greatest influence on the eigenfrequencies while removing the bass bar had the least impact. Yet, our hypothesis was not fully supported: not in all mode shapes did the original structure have the highest eigenfrequency value. Within the investigated components, we concluded that the factor affecting resonant vibration frequencies the most is Young's modulus, then soundpost, and, finally, the bass bar. Future research extension with physical experiments should be conducted to understand and quantify the result accuracy.

INTRODUCTION

Violins, a group of bowed instruments of the string family, are a universal yet versatile art form. The structural design of the violin – the bridge, the soundpost, and the bass bar – contributes to the resonance, the essence of the brilliance of violins' acoustics (1, 2). String instruments produce sound via vibrations, where sound waves travel through the wooden body, from the strings to the top and back plates through the bridge and soundpost (**Figure 1**) (3). Investigations of violin acoustics involve the specific frequencies that evoke unique vibrational shapes known as standing wave vibrations and Chladni patterns (4).

Chladni plates were invented by physicist and musician Ernst Chladni to demonstrate the patterns of standing wave vibrations (5). Under eigenfrequencies, frequencies at which the system is prone to vibrate in a specific shape called mode, the Chladni method rearranges the sprinkled particles into patterns depicting the nodal boundaries of the vibrating object (4, 6). Nodes are the areas where countering waves interfere destructively, staying at an equilibrium position, while the antinodes are the areas where the wave oscillates away from the equilibrium, with doubled amplitudes due to the traveling waves' constructive interference (7).

In an earlier Chladni method experiment on violin plates, a violin back was placed on a speaker with soft foam pads in between and aluminum flakes on the plate surface (8). The pads served to transfer the sound waves from the speaker to the plate, supporting the plate at a nodal point (8, 9). This allowed a visualization of the vibration, outlining the boundary configurations of a particular pitch. The rigorous bending motion moved the aluminum particles from antinodal toward nodal areas (8). Such frequencies forming the eigenmode are eigenfrequencies, which appear as standing waves in string instruments (4, 6, 8). One can analyze the resonance with eigenfrequency (quantified data). It is mainly studied in mechanical structures, where eigenfrequency vibrations create certain eigenmodes that the structure deforms into (6).

In a physical investigation with violin on its air and acoustic resonance, the researchers identified specific modes and eigenfrequencies. The primary mode shapes include one-sided and left and right halves vibration patterns (10). With the curiosity of investigating structurally altered cello models, another research duplicated these findings with simulations and further extended instrumental research (11). The soundpost and bass bar are two integral components of string instruments (12). The simulations of a violin's eigenfrequencies under different structures — central soundpost, no soundpost, no bass bar, etc. — revealed that the frequencies corresponding to the same mode shape increase as the model progresses from having no soundpost to centered soundpost and offset soundpost (original position) (11). The soundpost allowed flexural waves, which are bending waves transversely propagating through the medium, to flow between the top and bottom plates of the violin body (11, 13). As the soundpost moved away from the center, it increased the penetration of flexural waves around the spaces in between the two f-holes (**Figure 1**) (11,14). The waves also triggered horizontally asymmetric vibration modes (11,14). Eliminating the bass bar suggested that the bass bar couples the upper-lower bout vibrations (11,14). As a barrier to flexural wave displacement, the bass bar collaborated with the soundpost to break the symmetry constraints (11,14). The existence of the bass bar influenced the distribution of vibrational energy, which changed its resonance qualities (11,14). By "locking into" the upper and lower bouts, the bass bar's two ends introduced more localized vibrations, in turn, leading to the increase in eigenfrequencies (11,14). This research theorized

https://doi.org/10.59720/23-254

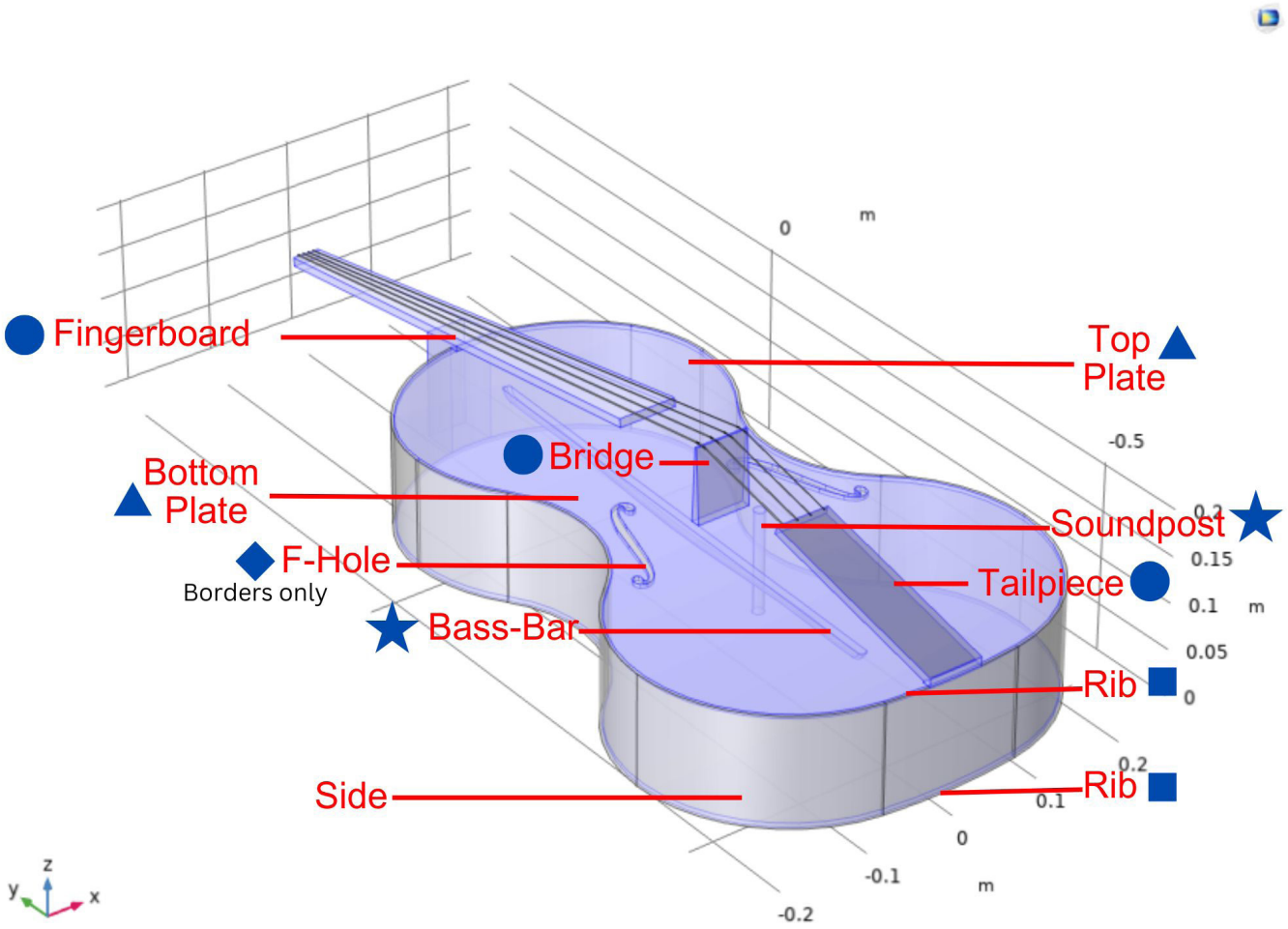

Figure 1: Cello anatomy and the cello geometry CAD file. The different parts of cello are shown and labeled. The dark blue shapes beside the cello parts categorize each part's domain setting in COMSOL Multiphysics®. A triangle (▲) represents a domain selection of "Solid Mechanics," "Linear Elastic Material, "Free" and "Initial Values." For stars (★), all of the above plus "Fixed Constraint – Boundaries" were selected. A circle (●) represents a domain selection similar to the stars, except "Free" was not included, and there was an additional selection of "Fixed Constraint – Domain." The rhombus (♦) indicates a single selection of "Free," while the square (■) means only "Fixed Constraint – Boundaries" was selected.

and explained observed phenomena that may be useful for analysis in our research.

In terms of Young's modulus, which is the elasticity of a solid undergoing tension, it determines the flexural wave's dispersion relationship, i.e., the relation between the wave's frequency and wavelength (15, 16, 17). This is extracted from the Kirchhoff-love plate theory, which models the deformation of a three-dimensional plate (16, 18). In theory, the eigenfrequency is dependent on the properties of the spruce material, including Young's modulus and Poisson's ratio (measure of deformation perpendicular to loading direction) (16).

Most previous research on string instruments focused on the violin. This experiment, instead, changed the subject to a cello to understand if differences in the plate thickness and dimensions, including length, width, and height, affect the resulting eigenfrequencies and mode shapes. We chose to investigate from a simulation approach, using COMSOL Multiphysics® Simulation, a simulation platform for simulating devices and designs in all fields of engineering, manufacturing, and scientific research (6). COMSOL Multiphysics® was chosen for its better affordability than most commercial finite element analysis (FEA) software, the abundance of accurately calculated values helpful for scientific analyses, and the flexibility in structural alterations (19). This software uses the finite element method (FEM) as the primary way to achieve an approximation based on discretization for partial differential equations (PDEs) (6). In other words, the PDEs numerically estimate a change in a system, solved with an estimation known as FEM with solutions at all positions (6). Discretization transfers continuous functions into discrete parts, which is superb for analyzing the sound modes of instruments that are time-dependent.

By using the COMSOL Multiphysics® simulation software, we altered the wood material's Young's modulus to understand the relation between material and acoustics properties (20). Changing the configurations of the soundpost and bass bar, we also investigated the structural mechanics versus acoustics characteristics. The purpose of this research is to uncover the physics behind cello acoustics while aiming to

https://doi.org/10.59720/23-254

Structural Models	Vibrational Mode Shape # with Eigenfrequency (Hz)					
	#1	#2	#3	#4	#5	#6
A. Original	268.5	339.0	470.5	481.7	557.0	
B. 12,000 MPa *E*	328.9	415.2	576.2	590.0	682.2	
C. No Soundpost	260.5	342.7	449.2	472.9		586.1
D. Centered Soundpost	254.0	345.2	467.1	539.4		561.0
E. No bass bar	268.5	339.0	470.5	458.5	557.4	596.6
(B) / (A) ratio	1.22	1.22	1.22	1.22	1.22	

Table 1: Resultant eigenfrequencies from structural models A-E. Statistical values of eigenfrequencies in Hz, as calculated using COMSOL Multiphysics®, summarized in a table, categorized by structural models and mode shapes. Mode Shapes that did not occur in certain structures are left blank in the table.

understand components' roles in instrument vibration. We assumed that eliminating components not made for sound optimization purposes would not affect the result accuracy. Following earlier observations, we hypothesized that the structural alterations will reflect in eigenfrequencies (11). We observed Young's modulus and soundpost to have a greater influence on the values than the bass bar. This proved that material choice's critical role in string instrument production and soundpost's relative importance in perfecting sound. The bass bar's presence, however, is of less importance to sound optimization. This research identified and proved the roles that each investigated factor plays in a cello, while also acknowledging their material and structural importance. By using the COMSOL Multiphysics®, this simulation is the pre-step to physical experiments. The presented findings demonstrated how solid mechanics, materials design, and computer-aided design can combine to predict the collective performance of a cello.

RESULTS

To find the eigenfrequencies of different structures, we set up the physics field in the software as "Solid Mechanics" with five models: Original, 12,000 MPa *E*, No soundpost, Centered Soundpost, No bass bar (**Table 1**) (11). The *standard set* is the "original" model, where components like soundpost and bass bar both exist and are off-set in their conventional positions, while the young's modulus is 8,000 MPa *E*, that of common cello-making wood materials like spruce or maple. We imported a self-drawn cello geometry CAD file with reference to Ref (20) and adjusted the components of the cello. The "Mode Shape" function allowed visualizations of the eigenmodes for each structural condition while showing the eigenfrequencies values in Hertz (Hz) (**Figure 2**). We classified the resultant vibration modes as *Mode #1-#6*, with different mode shapes showing the displacement magnitude of the front and back plate due to vibrations (**Figure 2**). Most of the resultant mode shapes matched the comparisons between simulation and real-life experiments from earlier studies, meaning that these simulation-based results could represent observations through physical investigation (10, 11, 21). We compared the results extracted from altered models to the standard set, where all the components resemble a physical cello design, for analysis.

Young's Modulus

As we changed the *E* value of the spruce that cover the front and back plates, bridge, rib, and tailpiece, from 8,000 MPa to 12,000 MPa, the resultant eigenfrequencies reflected a huge shift in results (**Table 1, Figure 3**). The difference ranged from 60 Hz (22.3%) to 125 Hz (22.4%) across the eigenmodes (**Table 1**). Additionally, we observed the values to have a scale factor relationship between the two models of approximately 1.22 for all modes (**Table 1**).

Soundpost

We further compared the standard set with models without a soundpost and a centered soundpost. The differences in eigenfrequencies varied with the eigenmode: modes *#1* and *#3* both had lower frequencies for the original structure than the other two soundpost alterations, while modes *#2* and *#4* had opposite results (**Table 1, Figure 3**). Generally, most modes were present regardless of the soundpost structural conditions, aligned with earlier findings (11). The missing mode *#5* data and the presence of mode *#6* were also notable since this change only happened when the soundpost was not in standard positions (**Table 1**). Only if the "no soundpost" and "centered soundpost" results were compared to the "12,000 MPa *E*" data set, were the latter's eigenfrequency always higher than that of altered models, matching earlier studies (11).

Bass Bar

The bass bar removal yielded minimal changes to the eigenfrequencies for each mode. Compared to the standard set, bass bar removal reflected an eigenfrequencies difference of 0 to 0.5 Hz (0-0.09%) for most modes. Only mode #4 demonstrated a 23 Hz (4.8%) difference, with minimal plate displacement (**Table 1**). These results are slightly different from an earlier observation of a 6% increase for bass bar addition (11). Eigenfrequencies of modes *#1~#3* stayed unchanged when the bass bar was added, while mode #4 had a 4.8% increase. Different from the results with soundpost structural alterations, a lack of bass bar gave rise to modes *#5* and *#6*.

DISCUSSION

We found that the structural change with Young's modulus, soundpost, and bass bar did affect the eigenfrequency, as hypothesized. The mode shapes mostly aligned with earlier studies' results, including physical experiments in Ref (10). Specifically, mode #4 was similar to the single-sided resonance, and mode #3 resembled the lower bout left and right halves pattern (10). Frequency-wise, eigenfrequencies in the present study are lower. This is because past studies used the violin as their experimental subjects, whose smaller body enabled resonance at higher frequencies compared to a cello (11). Due to fundamental differences in the instruments' dimensions, the following discussions solely compare the exhibited trends.

For the data set with *E* as the variable, the eigenfrequency of the 12,000 MPa *E* model had a 1.22 scale factor to that of the 8,000 MPa *E* model (**Table 1**). One potential explanation is the Kirchhoff-Love Plate Theory: the flexural wave's dispersion relationship is the product of vector *k* and a constant (16- 18).

https://doi.org/10.59720/23-254

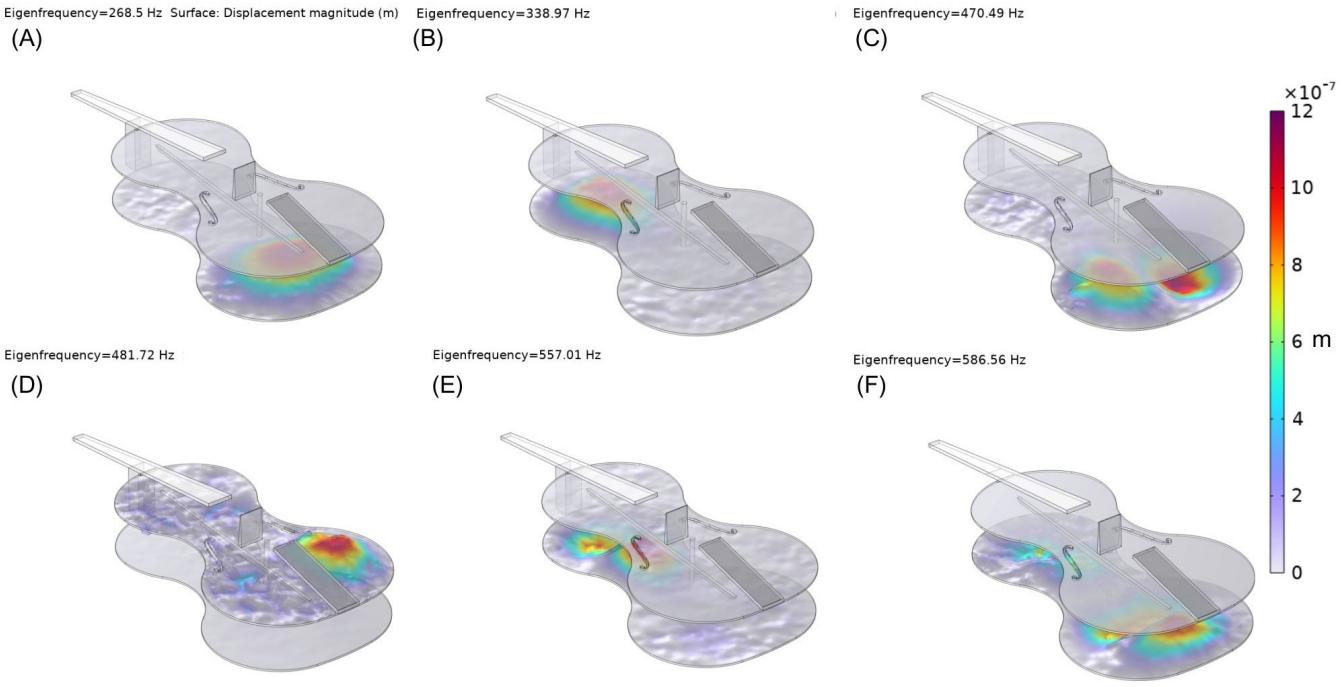

Figure 2: The frequencies and vibration mode shapes. (A) Mode #1 shape resulted from the original structure model with one bulge at the bottom plate lower bout. (B) Mode #2 shape with one bulge at the bottom plate upper bout. (C) Mode #3 shape with two opposite bulges at the bottom plate lower bout. (D) Mode #4 shape with one bulge at the right of the lower bout on the top plate. (E) Mode #5 shape with two bulges at the bottom plate upper bout. (F) Mode #6 shape resulted from the no soundpost structure model with four bulges at the bottom plate. The color bar indicates the displacement magnitude in meters.

$$f(k) = C \cdot k^2 \quad (1)$$

where vector *k* is the flexural wave's wave number, calculated by the reciprocal of wavelength (number of cycles per unit distance) (22). Meanwhile, the constant is calculated by

$$C = \frac{1}{2\pi}\sqrt{\frac{Ed^2}{12\rho(1-\nu^2)}} \quad (2)$$

where *E* is Young's modulus, *v* is Poisson's ratio, *p* is the mass density, and *d* is the thickness of the plate (16). As all variables except *E* were identical for both models, the *f*(*k*) ratio was 1.22, the scale factor relating to the eigenfrequency for all modes (**Table 1**).

This provides a potential explanation for the considerable difference in eigenfrequency between the standard and altered models, demonstrating the essential role of wood's Young's modulus in the cello's acoustics, as discussed by an earlier study (1). More evidence for the conformation to this rule can be obtained by changing the *E* value by finer increments. Another potential extension is to set the Poisson's ratio, mass density, and thickness of the plates as separate variables while keeping *E* constant. This could show how equations 1 and 2 accurately predict an instrument model's eigenfrequencies, proving *E* and eigenfrequency's relationship.

Moving on to structural changes with the soundpost, mode #6 only occurred when the model was not the standard set (**Table 1, Figure 3**). It was inferred that the soundpost's placement impacted the string instruments' sound projection. As early studies described, the soundpost connects the top and bottom plates (**Figure 1**), where the two contact points induce rigorous vibrations for flexural waves to penetrate the plates (11, 14). In this case, mode #6, with the four small bulges spanning across the back plate, occurred since there was not a soundpost, or it failed to transfer the flexural waves (energy) into one or two focused displacements.

The eigenfrequencies calculated for "original," "no soundpost," and "centered soundpost" mostly aligned with earlier findings, with some dissimilarities (**Table 1**) (11). For instance, adding a soundpost at the standard position increased the eigenfrequency for modes #1, #3, and #4 (11). Yet, the slight frequency decrease in #2 disarrayed from that conclusion (11). In addition, modes #2, #3, and #4 induced higher eigenfrequencies for a centered soundpost model compared to the original, similar to Ref (11). A lower frequency was observed for modes #1 and #6 for the same comparison, which were not discussed in earlier studies (11). Though the inconsistencies were minimal, some energies associated with sound transmission may have been consumed by additional structural parts in this model compared to other studies (including the neck, fingerboard, strings, bridge, and tailpiece), which lowered the frequencies (11, 21).

Interestingly, the results of the 12,000 MPa *E* model always had a higher eigenfrequency compared to the rest of the configurations. This finding is similar to earlier demonstrations

https://doi.org/10.59720/23-254

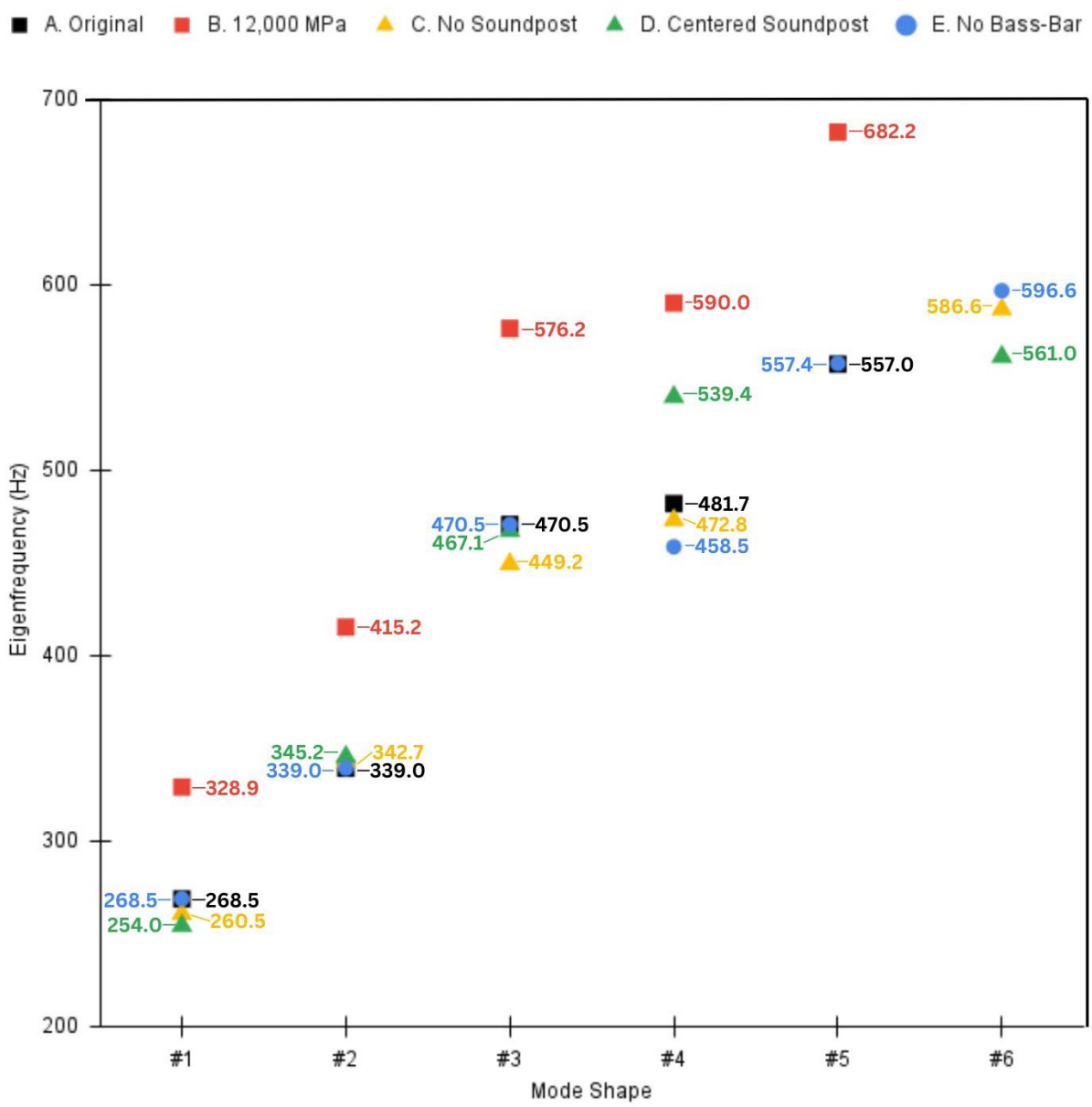

Figure 3: The eigenfrequencies calculated for different structural models. COMSOL Multiphysics® calculated the eigenfrequencies with each cello model's structure and material condition. The black square data points indicate the eigenfrequencies for a model with all components at their standard positions, while the values marked with red squares represent the model with a wood Young's modulus of 12,000 MPa. The yellow triangle dataset was from the model without a soundpost, and the green triangles indicate the model has a soundpost placed in the center. Lastly, the blue circles represent the eigenvalues calculated with a model without a bass bar.

and studies (11). Further investigations on the alteration of the cello structure with the 12,000MPa *E* Model should be conducted to determine if the cello completely follows the conclusion that a standard model's eigenfrequency is always higher than the rest of the configurations (11).

It was also observable that putting the soundpost at the original position prohibited mode #6's emergence, while displacing or removing it disallowed mode #5 (**Table 1**). Having soundpost in the middle or removing it allowed symmetrical, full-plate vibration, which is the case for mode #6 (**Figure 2**). However, if the soundpost was at the original position, it encouraged asymmetrical vibrational modes that do not cover the full plate, like mode #5 (**Table 1, Figure 2**) (11).

Finally, the bass bar is known to amplify the sound for string instruments by distributing the vibrations to the entire top plate (23). It is no surprise that the results showed minimal eigenfrequency changes with or without the bass bar, consistent with earlier conclusions (11). Though there was a slight difference in the displacement magnitude between modes (**Figure 2**), the eigenfrequency analysis in COMSOL Multiphysics® only drew the vibrational shapes but not the physical amplitudes of vibration (6). The magnitude of displacement simply indicates a material's resistance to structural vibrations (24). To determine the actual deformation scale, the materials' specific damping is required (6). For

https://doi.org/10.59720/23-254

materials having non-homogenous stress, their damping properties are mainly affected by the structure's geometry, like how cellos vary by geometry slightly (25). Extended research simulations with the damping properties considered should be conducted to understand the bass bar's relationship to string instruments.

The 5% increase in frequency for adding the bass bar was different from earlier observations of a 6% increase (11). Due to the energy conservation law, one reason may be that the additional cello parts consumed vibrational energy, which slightly affected the eigenfrequencies. The bass bar functions as an amplifier, as evidenced by the presence of mode *#5* with the bass bar removed: despite the absence of the bass bar, the shape of mode *#5* still resembled that of the standard model. However, the absence led to the emergence of mode #6. Removing the bass bar gave the upper and lower bout much more freedom, as the bass bar used to "lock in" the plates (11). This removed the constraints for full-plate vibration (11). In short, the existence of modes #5 and #6 existence for these models provide the bass bar's duality as an amplifier and a structural part to limit the upper-lower bouts vibration.

Overall, the results from the change in Young's modulus were most observable, suggesting the importance of wood choices in the optimization of string instruments' sound. While changes in soundpost positions also did affect eigenfrequencies, further investigations should be carried out to ensure a parallel conclusion with a violin. The bass bar, however, is mainly used to amplify the instrument's sound. This experiment concluded that wood material for the instrument body is a major factor in perfecting resonant vibration, while the components' positions relatively impact the sound characteristics. Yet, the components allowed asymmetrical and symmetrical flexural waves to flow through the two f-holes and interior body (11, 14, 21). The features each played a distinctive role in the cello instrument build-up. By comparing to the studies with violins, our simulations with a cello model noted the two's subtle differences and similarities.

As this study used a theoretical approach with simulated results, it was difficult to verify the accuracy of calculated eigenfrequencies and their relationships under material and structural changes. Furthermore, due to the software's limitations for the CAD file that required the entire instrument body to be drawn with a limited lines and that there should only be curved edges without sharp vertexes, the study was limited to investigating the simplified cello model with a uniformed *E* for all wood components (**Figure 1**), which may have led to unknown inaccuracies.

For future experiments, other than conducting physical investigations, the simulation's complexity could be increased by setting different parts of the instrument with corresponding wood material's *E*, which is closer to a real-life cello. Material properties such as the Poisson's ratio of the wood can also be taken into consideration, as it showed a strong relation with eigenfrequencies according to the Kirchhoff-Love Plate Theory. Future topics for investigation also include changing the shape of the f-holes. A simulation work based on the violin model showed that the area of the void decreased as the perimeter of the shape increased, which enabled and maximized the sound flow (2). Investigating the same topic on a cello model would further reveal the violin and the cello's resemblance and differences.

MATERIALS AND METHODS

Computer-Aided Design

Using the CAD tool Parametric Technology Corporation Creo (26), with reference to the dimensions of the cello CAD file from GrabCAD® by Eric Slotty (20), we drew a simplified cello model to accommodate COMSOL Multiphysics®'s curvature and segment restrictions. The simplified geometry still included components like the neck, fingerboard, side, top and bottom plate, f-holes, bridge, soundpost, and bass bar, and a tailpiece simplified into a rectangular prism (**Figure 1**). The f-holes and other components remained detailed since they are essential to an instrument's resonance (2, 21). In addition, we flattened the curvature of the top and bottom plates for simpler calculations. Plus, it is less important as the frequency rises (27).

Setting up Cello Model in COMSOL Multiphysics®

After the CAD file was imported, the "Materials" of the cello body was set as "Spruce." We set the f-hole openings as "Air," similar to the setup in COMSOL Multiphysics®'s example of "Violin Resonance" (28). For this simulation, the physics field of "Solid Mechanics" was selected with all components from the geometry except the rib of the cello body for "domain selection," as demonstrated in the same simulation with a violin (**Figure 1**). We selected the linear elastic material for all components except the rib. Under this setting page, we specified the *E* of wood components to 8 GPa by referring to the common cello-making wood materials. Simulated and experimentally determined Young's moduli of the violin's plates have been reported to be 12.6 and 9.9 GPa (1). These values are close to common wood materials for making violins, such as spruce (approximately 7.5 to 9.5 GPa) and maple (approximately 10.7 to 12.6 GPa) (1, 11, 29, 30). On the other hand, the Poisson's ratio and density were set as 0.57 and 500 kg/m^3, respectively. For free boundaries, only the domains except for components on top of the plate were included. While the "Initial Values" remained the same, a "fixed constraint" on "edges" was added and selected for the rib border and all components' borders to avoid unrealistic deformation due to vibration. We also included another "fixed constraint" on "boundaries" to ensure the components above the front plate do not fly off the cello body. The final step for setup was to create the "Mesh" with "physics-controlled mesh." To calculate the resonant vibration frequencies, we selected "Eigenfrequencies" in the "Study" tab with a specification on searching for results around 200 Hz. Lastly, for structural alteration purposes, we repeated the entire process with a change in *E* value to 12 GPa, the removal of the soundpost, the shift of the soundpost to the center, and the removal of the bass bar.

Computation and Post-Processing

As simulated results do not vary across trials, the simulation for each configuration was run once. The diagrams of different eigenfrequencies and eigenmodes (**Figure 2**) were plotted and exploited. We observed the trends and changes that structure alterations introduced (**Figure 3**).

ACKNOWLEDGEMENTS

The author's first and foremost acknowledgment is dedicated to her cello teacher Ms. Janet Chien for her patience and devotion in years of teaching, as well as the

https://doi.org/10.59720/23-254

discussions made regarding this research. The authors are also grateful to receive help from Cheng, Chin-Yuan (Sarty), the Design and Service Engineering Lead of FIH, for assisting the CAD file drawing. Meaningful consultations with Tseng, Chih-Sheng (Gavin), the Acoustic Design Engineering Lead of FIH, are also gratefully acknowledged. In addition, the guidance from Pitotech Assistant Vice President Chun-Shan Tsui (Pavel) and its Equipment Engineering Division Assistant Manager Ku-Shen Lin (Amos) along the research process is highly appreciated. The authors would finally like to thank the National Science and Technology Council (Project No. NSTC 111-2224-E-002-007) for funding the usage of COMSOL Multiphysics® software.

Received: October 3, 2023
Accepted: February 11, 2024
Published: February 4, 2025

REFERENCES

1. Yokoyama, M. "Coupled Numerical Simulations of the Structure and Acoustics of a Violin Body." *The Journal of Acoustical Society of America*, vol.150, no.3, pp. 2058-2064, 2021. https://doi.org/10.1121/10.0006387.
2. Nia, H. T., *et al.* "The Evolution of Air Resonance Power Efficiency in the Violin and its Ancestors." *Proceedings of the Royal Society A,* vol. 471, no. 2175, 08 Mar. 2015, p. 20140905. https://doi.org/10.1098/rspa.2014.0905.
3. Kim, G. "VIOLIN - MAIN FUNCTIONAL REQUIREMENT: Create and Resonate (Hopefully Pleasant) Sound Waves." *Massachusetts Institute of Technology*. web.mit.edu/2.972/www/reports/violin/violin.html. Accessed 6 Jan. 2024.
4. "Chladni Plates." *Harvard University.* sciencedemonstrations.fas.harvard.edu/presentations/chladni-plates. Accessed 29 Sep. 2023.
5. Rees, T. "Ernst Chladni: Physicist, Musician and Musical Instrument Maker." *University of Cambridge*, 2009. www.whipplemuseum.cam.ac.uk/explore-whipple-collections/acoustics/ernst-chladni-physicist-musician-and-musical-instrument-maker. Accessed 17 Sep. 2023.
6. "COMSOL Documentation." *COMSOL Multiphysics®.* doc.comsol.com/6.1/docserver/#!/com.comsol.help.comsol/helpdesk/helpdesk.html. Accessed 29 Sep. 2023.
7. Zhabinskaya, D. "8.8: Standing Waves." *LibreTexts PHYSICS, UC Davis.* phys.libretexts.org/Courses/University_of_California_Davis/UCD%3A_Physics_7C_-_General_Physics/8%3A_Waves/8.8%3A_Standing_Waves. Accessed 6 Jan. 2024.
8. Hutchins, C. M. "The Acoustics of Violin Plates." *Scientific American*, vol. 245, no. 4, pp.170-180, 01 Oct. 1981. https://doi.org/10.1038/scientificamerican1081-170.
9. Ewins, D. J. "Mode of Vibration." *Encyclopedia of Vibration,* Elsevier, pp. 838-844, 2001. https://doi.org/10.1006/rwvb.2001.0062.
10. Runnemalm, A., *et al.* "On operating deflection shapes of the violin body including in-plane motions." *The Journal of the Acoustical Society of America*, vol. 107, no. 6, pp. 3452–3459, Jul. 2000. https://doi.org/10.1121/1.429415.
11. Gough, C. "Violin Plate Modes." *The Journal of the Acoustical Society of America,* vol. 137, no.1, pp. 139-153, 2015. https://doi.org/10.1121/1.4904544.
12. Savart, F. "Memoires sur le construction des Instruments a Cordes et a Archet" ("Submissions on the construction of string instruments and bow") *University of Lausanne & Roret Encyclopedic Bookstore,* 1819.
13. Hembric, S. A. "Structural Acoustics Tutorial—Part 1: Vibrations in Structures." *The Pennsylvania State University.* www.docenti.unina.it/webdocenti-be/allegati/materiale-didattico/129193. Accessed 6 Jan. 2024.
14. Gough, C. "The Violin Bridge-Island Input Filter." *The Journal of the Acoustical Society of America*, vol. 120, no. 1, pp. 482-491, Jan. 2018. https://doi.org/10.1121/1.5019474.
15. Hosch, W. L. "Young's Modulus." *Encyclopaedia Britannica.* www.britannica.com/science/Youngs-modulus. Accessed 6 Jan. 2024.
16. Tuan, P. H., *et al.* "Exploring the resonant vibration of thin plates: Reconstruction of Chladni patterns and determination of resonant wave numbers." *The Journal of the Acoustical Society of America*, vol. 137, no. 4, pp. 2113-2123, Apr. 2015. https://doi.org/10.1121/1.4916704.
17. Morin, D. "Dispersion." *Harvard University.* scholar.harvard.edu/files/david-morin/files/waves_dispersion.pdf. Accessed 6 Jan. 2024.
18. Ozenda, O. and E. G. Virga "On the Kirchhoff-Love Hypothesis (Revised and Vindicated)." *Journal of Elasticity*, vol. 143, pp. 359-384, 11 Feb. 2021. https://doi.org/10.1007/s10659-021-09819-7.
19. COMSOL Multiphysics® v. 6.1. www.comsol.com. COMSOL AB, Stockholm, Sweden.
20. Slotty, E. "A full size (755mm) cello assembly." *GrabCAD, Stratasys Inc.*, 28 Feb. 2020. grabcad.com/library/a-full-size-755mm-cello-assembly-1. Accessed 10 Oct. 2022.
21. Gough, C. "A Violin Shell Model: Vibrational Modes and Acoustics." *The Journal of the Acoustical Society of America,* vol. 137, no. 3, pp.1210-1225, Mar. 2015. https://doi.org/10.1121/1.4913458.
22. Elster, A. D. "The Meaning of 'k'." *Elster LLC, MRIquestions.* mriquestions.com/what-does-k-stand-for.html. Accessed 6 Jan. 2024.
23. McKean, J. "The Role (and Romance) of the bass bar." *STRINGS*, 28 Jun. 2016. stringsmagazine.com/the-role-and-romance-of-the-bass bar/. Accessed 17 Sep. 2023.
24. Bala, A. "Thermal resistivity, sound absorption and vibration damping of concrete composite doped with waste tire Rubber: A review." *Construction and Building Materials*, vol. 299, Sep. 2021. https://doi.org/10.1016/j.conbuildmat.2021.123939.
25. Orban, F. "Damping of materials and members in structures." *Journal of Physics: Conference Series*, vol. 268, 2011, p. 012022. https://doi.org/10.1088/1742-6596/268/1/012022.
26. Pro/ENGINEER®. www.proengineer.com/. Creo. Arizona, United States of America.
27. Cremer, L. *The Physics of the Violin.* Translated by J. S. Allen. Cambridge, Massachusetts, MIT Press, 14 Nov. 1983.
28. COMSOL. "Application Gallery." www.comsol.com/models. Application ID for Chladni Plate and Violin Acoustic-Structure Interaction examples are 67591 and 34861, respectively. Accessed 24 Mar. 2023.
29. Göken, J., *et al.* "Damping of Spruce Wood at Different Strain Amplitudes, Temperatures and Moisture Contents." *Romanian Journal of Physics*, vol. 68, no. 903, 2023. rjp.

https://doi.org/10.59720/23-254

nipne.ro/2023_68_1-2/RomJPhys.68.903.pdf.
30. AmesWeb. "Young's Modulus (Modulus of Elasticity) of Wood." *AmesWeb.* amesweb.info/Materials/Youngs-Modulus-of-Wood.aspx. Accessed 6 Jan. 2024.